VALIDATION OF MINIMUM-ENERGY BAND-LIMITED PREDICTION USING VEHICULAR CHANNEL MEASUREMENTS

Thomas Zemen[1], *Sebastian Caban*[2], *Nicolai Czink*[1,3] *and Markus Rupp*[2]

[1]ftw. Forschungszentrum Telekommunikation Wien
Donau-City-Straße 1, 1220 Vienna, Austria
email: thomas.zemen@ftw.at
http://userver.ftw.at/ zemen/

[2]Institute of Communications and Radio-Frequency Engineering, Vienna University of Technology
Gusshausstr. 25/389, 1010 Vienna, Austria

[3]Smart Antennas Research Group, Information Systems Lab, Stanford University
Packard 215, Stanford, CA 94305, USA

ABSTRACT

We demonstrate that minimum-energy (ME) band-limited prediction shows the same robust performance for vehicular channel measurements as well as for the numeric Clarke channel model. By contrast, channel prediction based on sinusoidal modelling presented by Chen et al., 2007, shows poor performance for a small percentage of measured channel realizations. This increases the mean square error dramatically, hence *outlier removal is required*. The ME band-limited predictor introduced by Zemen et al., 2007, is based on a subspace spanned by time-concentrated and band-limited sequences. The time-concentration of these sequences is matched to the length of the observation interval and the band-limitation is determined by the support of the Doppler power spectral density of the fading process. The low-complexity time-variant flat-fading channel predictor dynamically selects a predefined subspace from a small set such that the prediction error is minimized. We validate the ME band-limited predictor using channel measurements from an alpine region. The predictor performance with measured channels is comparable to the one obtained with Clarke's channel model for non line-of-sight situations. For line-of-sight situations the performance is better than for Clarke's model. We present results in terms of mean square error averaged over *all* measured snapshots.

1. INTRODUCTION

In mobile communication systems channel state information at the transmitter proves to be beneficial for increasing the system capacity. In a time-division duplex (TDD) system channel state information can be obtained by exploiting channel reciprocity: While a data block is received, channel state information is obtained. This information can be utilized in the following transmission period. However, for moving users at vehicular speed the channel state information gets outdated rapidly. Thus, appropriate channel prediction is necessary.

In [1] Zemen et al. present a new minimum-energy (ME) band-limited prediction algorithm. This algorithm allows for low-complexity prediction of a fading process from noisy channel observations that are obtained while receiving a *single* data block. The symbol rate, or equivalently the sampling rate of the fading process, in wireless communication systems is much higher than the Doppler bandwidth. Thus, time-limited snapshots of the sampled fading process span a subspace with small dimension [2].

In [1] it is shown that a time-concentrated and band-limited sequence can be defined for generalized band-limits consisting of disjoint intervalls matching the support of the Doppler power spectral density of the time-selective fading process. The energy of these sequences is most concentrated in an interval equal to the length of the observed data block. Thus, they allow to calculate the ME band-limited continuation of a finite sequence [2], hence *predict* future samples. In [1] the algorithm is validated by the numeric Clarke model, only.

In [3] a prediction algorithm based on sinusoidal modeling is presented by Chen et al. It is shown that channel prediction based on sinusoidal modelling performs poor for a small number of *measured* channel realizations [3, Sect. 6]. This increases the mean square error (MSE) dramatically. Hence, [3] performs outlier removal and results are presented in terms of MSE with a given level of confidence. An enhanced approach utilizing multicomponent polynomial phase signals is presented in [4], however outlier removal is still required.

Contribution of this paper: In this paper the ME band-limited prediction algorithm with dynamic subspace selection is validated with vehicular channel measurements. We demonstrate the robustness of our algorithm. No outlier removal or other preprocessing is necessary for consistent performance on a large number of measured vehicular channel samples for line-of-sight (LOS) and non-LOS scenarios.

Organization of the paper: In Section 2 we introduce the signal model for time-variant flat-fading channels. The ME band-limited prediction algorithm [1] is shortly reviewed in Section 3 and the dynamic subspace selection in Section 4, respectively. Section 5 decribes the vehicular measurement scenario and the post-processing is discussed in Section 6. We present the simulation results in Section 7 and draw conclusions in Section 8.

Notation: We denote a column vector by $\boldsymbol{a}$ and its i-th element with $a[i]$. Similarly, we denote a matrix by $\boldsymbol{A}$ and its (i,ℓ)-th element by $[\boldsymbol{A}]_{i,\ell}$. The transpose of $\boldsymbol{A}$ is given by $\boldsymbol{A}^{\mathrm{T}}$ and its conjugate transpose by $\boldsymbol{A}^{\mathrm{H}}$. The absolute value of a is denoted by $|a|$ and its complex conjugate by a^*. The largest (smallest) integer that is lower (greater) or equal than $a \in \mathbb{R}$ is denoted by $\lfloor a \rfloor$ ($\lceil a \rceil$). We denote the set of all integers by $\mathbb{Z}$, the set of real numbers by $\mathbb{R}$ and the set of complex numbers by $\mathbb{C}$.

2. SIGNAL MODEL FOR TIME-VARIANT FLAT-FADING CHANNELS

We consider a time division duplex (TDD) communication system transmitting data in blocks of length M over a time-variant channel. The symbol duration T_S is much longer than the delay spread T_D of the channel, i.e., $T_S \gg T_D$. Hence we assume the channel as frequency-flat. Discrete time at rate $R_S = 1/T_S$ is denoted by m. The channel incorporates the transmit filter, the transmit antenna, the physical channel, the receive antenna, and the receive matched filter. The data symbols $b[m]$ are randomly and evenly drawn from a symbol alphabet with constant modulus. Without loss of generality $|b[m]| = 1$. The discrete-time signal at the matched filter output $h[m]b[m] + n'[m]$ is the superposition of the data symbol multiplied by the sampled time-variant channel weight $h[m]$ and complex white Gaussian noise $n'[m]$ with variance σ_n^2. Without loss of generality $\{h[m]\}$ is a circularly symmetric, unit-variance (due to power control) process.

We assume an error-free decision feedback structure [5]. Thus, we are able to obtain noisy channel observations [6] using the error-free data symbol estimates $\hat{b}[m] = b[m]$:

$$y[m] = h[m] + n[m]\,. \tag{1}$$

Note that $n[m]$ has the same statistical properties as $n'[m]$. The signal-to-noise ratio (SNR) is $\mathrm{SNR} = 1/\sigma_n^2$.

The transmission is block oriented. A data block spans the time interval $\mathscr{I}_M = \{0,\ldots,M-1\}$. The noisy channel observations $y[m]$, $m \in \mathscr{I}_M$ obtained during a single data block are used to predict the channel weight up to N symbols into the future.

For a user moving with velocity v the time-variant fading process $\{h[m]\}$ is band-limited by the one-sided normalized Doppler bandwidth

$$\nu_D = \frac{v f_C}{c_0} T_S \ll \frac{1}{2} \tag{2}$$

where f_C is the carrier frequency and c_0 stands for the speed of light. As indicated with the inequality in (2) the sampling rate $1/T_S$ is much higher than the Nyquist sampling rate.

We assume a time-variant block-fading channel model. Hence the fading process $\{h[m]\}$ is wide-sense stationary over the limited time interval $\mathscr{I}_{M+N}$ with covariance function

$$R_h[k] = \mathsf{E}\{h^*[m]h[m+k]\}\,. \tag{3}$$

3. MINIMUM-ENERGY (ME) BAND-LIMITED PREDICTION

The samples of the channel weights in a single block $\mathscr{I}_M$ are collected in the vector

$$\boldsymbol{h} = [h[0], h[1], \ldots, h[M-1]]^{\mathrm{T}}\,. \tag{4}$$

We consider a subspace-based approximation which expands the vector $\boldsymbol{h}$ in terms of D orthonormal basis vectors $\boldsymbol{u}_i = [u_i[0], u_i[1], \ldots, u_i[M-1]]^{\mathrm{T}}$, $i \in \{0,\ldots,D-1\}$:

$$\boldsymbol{h} \approx \boldsymbol{U}\boldsymbol{\gamma} = \sum_{i=0}^{D-1} \gamma_i \boldsymbol{u}_i\,. \tag{5}$$

In this expression $\boldsymbol{U} = [\boldsymbol{u}_0,\ldots,\boldsymbol{u}_{D-1}]$ contains the orthonormal basis vectors and $\boldsymbol{\gamma} = [\gamma_0,\ldots,\gamma_{D-1}]^{\mathrm{T}}$ collects the basis expansion coefficients. The least square estimate of $\boldsymbol{\gamma}$ simplifies to

$$\hat{\boldsymbol{\gamma}} = \boldsymbol{U}^{\mathrm{H}}\boldsymbol{y} \tag{6}$$

due to the orthogonality of the basis functions. The reconstruction error per data block is defined as

$$z = \frac{1}{M}\|\boldsymbol{h} - \boldsymbol{U}\hat{\boldsymbol{\gamma}}\|^2\,. \tag{7}$$

We define the mean square reconstruction error per sample

$$\mathrm{MSE}[m] = \mathsf{E}\left\{|h[m] - \hat{h}[m]|^2\right\}, \tag{8}$$

and the mean square reconstruction error per data block,

$$\mathrm{MSE} = \frac{D}{M}\sigma_n^2 + \frac{1}{M}\mathsf{E}\{\|\boldsymbol{V}^{\mathrm{H}}\boldsymbol{h}\|^2\}, \tag{9}$$

where $\boldsymbol{V} = [\boldsymbol{u}_D,\ldots,\boldsymbol{u}_{M-1}]$ contains the basis vectors spanning the subspace orthogonal to the signal subspace spanned by the columns of $\boldsymbol{U}$. The noise samples are collected in the vector $\boldsymbol{n} = [n[0],\ldots,n[M-1]]^{\mathrm{T}}$. We seek basis vectors $\boldsymbol{u}_0,\ldots,\boldsymbol{u}_{D-1}$ and the subspace dimension D which minimize the reconstruction error per data block.

In mobile radio-communication channels, the most significant part of the power in the estimated Doppler spectrum of the fading process is usually localized on the union of disjoint intervals in the frequency range $(-1/2,+1/2)$. A region $\mathscr{W} \subseteq (-1/2,1/2)$ consisting of I disjoint intervals $\mathscr{B}_i = (\nu_{i1},\nu_{i2})$, $i \in \{1,\ldots,I\}$ can be defined as

$$\mathscr{W} = \bigcup_{i=1}^{I} \mathscr{B}_i = \mathscr{B}_1 \cup \mathscr{B}_2 \cup \ldots \cup \mathscr{B}_I\,, \tag{10}$$

with $\nu_{11} \le \nu_{12} \le \ldots \le \nu_{I1} \le \nu_{I2}$, see [1, Fig. 1].

The sequences $\{u_i[m,\mathscr{W}]\}$, $i \in \{0,\ldots,M-1\}$ band-limited to the region $\mathscr{W}$ and with *most concentrated* energy in the interval $\mathscr{I}_M$ are the solutions to

$$\sum_{\ell=0}^{M-1} C[\ell-m,\mathscr{W}]u_i[\ell,\mathscr{W}] = \lambda_i(\mathscr{W})u_i[m,\mathscr{W}]\,, \quad m \in \mathbb{Z} \tag{11}$$

where

$$C[k,\mathscr{W}] = \int_{\mathscr{W}} \mathrm{e}^{\mathrm{j}2\pi k\nu}\mathrm{d}\nu\,. \tag{12}$$

Note that $C[k,\mathscr{W}]$ is proportional to the covariance function of a process exhibiting a constant spectrum with support $\mathscr{W}$. For more details please refer to [1].

The ME band-limited prediction of a time-variant channel for any $m \in \mathbb{Z}$ can be expressed as [1]

$$\hat{h}[m] = \boldsymbol{f}[m,\mathscr{W}]^{\mathrm{T}}\hat{\boldsymbol{\gamma}} = \sum_{i=0}^{D(\mathscr{W})-1} \hat{\gamma}_i u_i[m,\mathscr{W}]\,, \tag{13}$$

where $\boldsymbol{f}[m,\mathscr{W}] = [u_0[m,\mathscr{W}],\ldots,u_{D(\mathscr{W})-1}[m,\mathscr{W}]]^{\mathrm{T}}$.

4. SUBSPACE DEFINITION AND DYNAMIC SELECTION

In practical systems information about the Doppler bandwidth must be obtained from channel observations. We define a finite number of hypotheses about the actual Doppler

Figure 1: The alpine measurement scenario.

bandwidth. Each hypothesis is represented by a subspace spanned by time-concentrated and band-limited sequences. The orthogonal basis vectors spanning each subspace are calculated once and then stored. A subspace selection method based on a probabilistic bound on the reconstruction error z (7) is used to select the subspace with the smallest reconstruction error based on the observation of a single data block. This subspace is used for ME band-limited prediction.

4.1 Subspace Definition

We define the maximum Doppler bandwidth

$$\nu_{\text{Dmax}} = \frac{v_{\max} f_{\text{C}} T_{\text{S}}}{c_0} \tag{14}$$

as system parameter given by the maximum (supported) user velocity $v_{\max}$. Furthermore, we define a set of Q subspaces with spectral support

$$\mathscr{W}_q = \left(-\frac{q}{Q}\nu_{\text{Dmax}}, +\frac{q}{Q}\nu_{\text{Dmax}}\right) \tag{15}$$

for $q \in \{1, \ldots, Q\}$ as shown in [1, Fig. 3].

In mobile communication channels, fading processes frequently arise whose spectral support is the union of disjoint intervals. Hence we define an additional set of subspaces by partitioning the region $(-\nu_{\text{Dmax}}, \nu_{\text{Dmax}})$ into Q' spectral bins with equal length as depicted in [1, Fig. 4].

The spectral bin $i \in \{1, \ldots, Q'\}$ spans the interval

$$\mathscr{B}_i = \left[-\nu_{\text{Dmax}} + (i-1)\frac{\nu_{\text{Dmax}}}{Q'}, -\nu_{\text{Dmax}} + i\frac{\nu_{\text{Dmax}}}{Q'}\right]. \tag{16}$$

Using all possible binary combinations of $\mathscr{B}_i$ we can define $2^{Q'}-1$ band-limiting regions $\mathscr{W}'_{q'}$, $q' \in \{1, \ldots, 2^{Q'}-1\}$.

We combine the set of symmetric subspace $\boldsymbol{U}_q$ with $Q = 10$ and the set of asymmetric subspaces $\boldsymbol{U}'_{q'}$, $q' \in \{1, \ldots, 2^{Q'}-1\}$ with $Q' = 4$ leaving out duplicates.

4.2 Subspace Selection

In [7] an information theoretic subspace selection scheme is proposed. This method uses the observable data error

$$x_q = \frac{1}{M}\|\boldsymbol{y} - \boldsymbol{U}_q \boldsymbol{U}_q^{\text{H}} \boldsymbol{y}\|^2 \tag{17}$$

to obtain an upper bound $\overline{z_q}(x_q)$ on the reconstruction error

$$z_q = \frac{1}{M}\|\boldsymbol{h} - \hat{\boldsymbol{h}}_q\|^2 \le \overline{z_q}(x_q) \tag{18}$$

which cannot be observed directly. For the subspace selection $\boldsymbol{h}$ is considered deterministic. The results in [7] are derived for real valued signals. They are adapted for complex valued signals and noise in [1].

The upper bound on the reconstruction error is used to select the appropriate subspace q spanned by the columns of $\boldsymbol{U}_q$,

$$\hat{q} = \underset{q}{\operatorname{argmin}}\, \overline{z_q}(x_q). \tag{19}$$

The chosen subspace $\boldsymbol{U}_{\hat{q}}$ and the associated sequences $\{u_i[m, \mathscr{W}_q]\}$ are used for ME band-limited prediction [1].

5. VEHICULAR CHANNEL MEASUREMENTS

To validate the prediction algorithm we use outdoor vehicular channel measurements carried out in the alpine Drautal valley in Austria. The basic set-up of the Vienna MIMO Testbed [8] is as follows:

- A base station is set up at one side of the Drautal valley right next to already existing base stations. Exactly every 500 ms it transmits a frame with the following parameters:
  - 100 ms duration
  - 4-quadrature amplitude modulated (QAM) single carrier signal (511 training symbols and $S = 1000$ data symbols), root-raiced-cosine (RRC) filtered with a roll-off factor of 0.5
  - 15 kHz bandwidth[1], resulting in $T_{\text{S}} = 66.7\ \mu$s.
  - $f_{\text{C}} = 2.5$ GHz center frequency (the wavelength is approx. 12 cm)
  - 37 dBm TX power

  We employ a Kathrein 800 10543 base station antenna [9] with $+45^\circ$ polarization, half-power beam width $58^\circ/6.2^\circ$ and down tilt 6°.

- The corresponding receiver is placed in a "VW-Sprinter" van that follows a route through the valley. Four receive antennas were placed in front of the passenger seat as depicted in Figure 1. For the analysis in this paper only one antenna is used.

Prior to the actual measurement, the TX and RX-unit were synchronized relative to each other (see [10] for more details). This initial synchronization was then maintained throughout the whole measurement to ensure perfect timing and frequency synchronization of the received frame (see Figure 2).

[1] chosen similar to the orthogonal frequency division multiplexing (OFDM) subcarrier bandwidth in UMTS long term evolution (LTE)

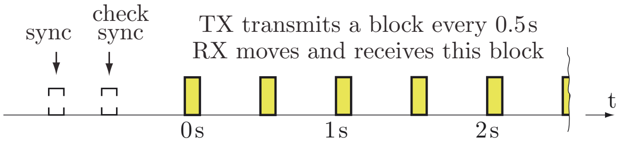

Figure 2: Timing diagram.

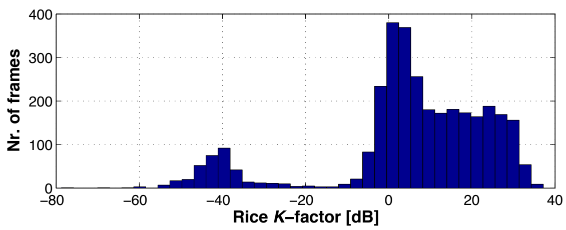

Figure 3: Histogram of Rice K-factor (in dB) for all measured frames.

During the actual measurement, the receiver captured the frames transmitted by the base-station and stores them on a hard-disk. These stored complex baseband-data samples are the input to all off-line evaluations carried out later.

6. POST-PROCESSING

For post-processing the received signal baseband samples are RRC filtered and synchronized in time by correlating with the training symbol sequence.

During the measurement drive with a duration of approximately half an hour a total number of $F = 3171$ frames were received. The propagation condition varied from line-of-sight (LOS) on a rural road to non-LOS within villages. In Figure 3 we plot a histogram showing the histogram of the Rice K-factor in dB. For the Rice K-factor estimation we used the method of moments [11] as initial guess for a least squares fit of the Rice probability density function (pdf). The Kolmogorov-Smirnov goodness of fit [12, pp. 392–394] is depicted in Figure 4. Hence, the largest distance between the Rice cumulative distribution function (cdf) and the empirical cdf is smaller than 0.1 for 90% of all measurement frames.

The histogram of SNR is depicted in Figure 5. The SNR of 95% of all snapshots is above 25 dB. Due to the high SNR for all frames we can treat the obtained channel sample as perfect channel knowledge $h_f[m]$ where $0 \leq f \leq F-1$ and $0 \leq m \leq S-1$. The frame index is denoted by f.

Finally, the velocity histogram is shown in Figure 6. The velocity per frame is obtained from the collected GPS data

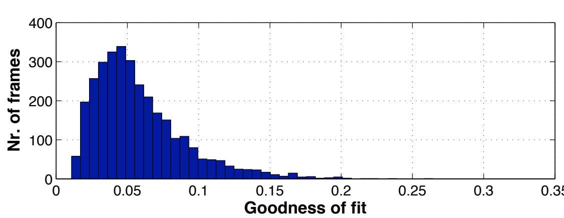

Figure 4: Histogram of Kolmogorov-Smirnov goodness of fit for Rice pdf for all measured frames.

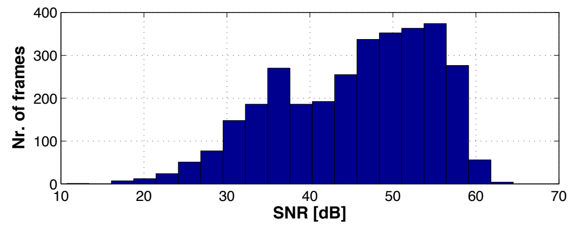

Figure 5: Histogram of SNR for all measured frames.

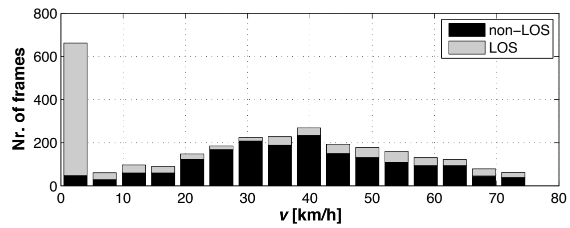

Figure 6: Histogram of velocity for measured LOS frames ($K_f \leq 10$) and non-LOS frames ($K_f > 10$).

collected during the measurement. We show the number of frames per velocity bin with non-LOS conditions for $K_f \leq 10$ (black) and LOS conditions with $K_f > 10$ (light gray). We take all snapshots into account with a velocity $v \leq 80$ km/h. This is done to ensure a sufficiently large set of frames per evaluated velocity bin for later statistical evaluations. For easier comparison with [1] we keep $v_{\max} = 100$ km/h.

Each frame is normalized such that $\mathsf{E}\{|h_f[m]|^2\} = 1$. Finally, we add complex white Gaussian noise noise $n_f[m] \sim \mathcal{N}(0, \sigma_n^2)$ with $\sigma_n^2 = 0.1$ resulting in a SNR = 10 dB obtaining noisy channel observations $y_f[m]$ according to (1) with defined properties.

7. SIMULATION RESULTS

We are interested to investigate the performance of ME band-limited prediction with dynamic subspace selection in realistic channel conditions.

We need to adapt the results from [1] to the symbol duration $T_S = 66.67\,\mu$s of our vehicular measurements. In [1] a symbol duration of 20.57μs is used. We keep the assumption that the predictor is able to observe the channel at most for the duration of two wavelengths at a velocity of $v_{\max} = 100$ km/h resulting in a block length of $M = 128$. We will analyze two prediction horizons, namely $\ell \in \{8, 24\}$ (equivalent to $\{\lambda/8, 3\lambda/8\}$ at $v_{\max}$.).

As base-line performance we use Monte-Carlo simulation with Clarke's channel model [13]. The Clarke model with $P = 30$ scatterers is representative for non-LOS situations with rich scattering. These results are compared with the one for noisy channel observations $y_f[m]$ obtained from vehicular channel measurements. We will distinguish two cases, namely the quasi non-LOS case characterized by $K_f \leq 10$ and the LOS case with $K_f > 10$.

In Figure 7 we plot MSE$[M-1+\ell]$ versus the normalized Doppler bandwidth ν_D for a velocity range $0 \leq v \leq 80$ km/h. The predictor performance with measured channels is slightly worse in the non-LOS case (especially for small velocities) compared to Clarke's model. In the LOS case

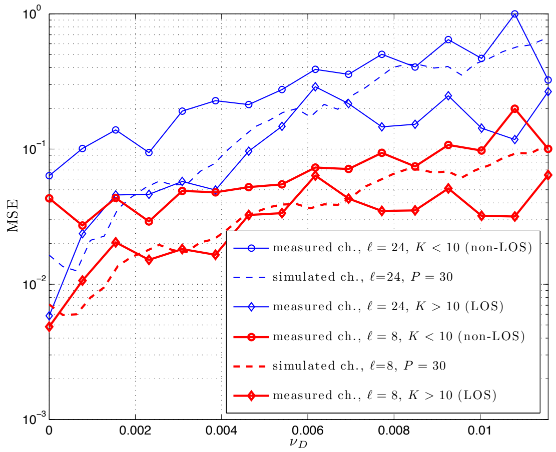

Figure 7: Mean square prediction error versus normalized Doppler bandwidth. We compare the prediction performance for measured vehicular channels with the one for the numeric Clarke channel model. Two prediction horizons $\ell \in \{8,24\}$ are evaluated (equivalent to $\{\lambda/8, 3\lambda/8\}$ at $v_{\max}$).

the performance is better than the one obtained with Clarke's model. We emphasize that this result clearly shows the robustness of ME band-limited prediction with dynamic subspace selection. No outlier removal is required (compared to the results in [3]).

8. CONCLUSIONS

In this paper we validated the minimum-energy (ME) band-limited prediction method [1] comparing performance results for vehicular channel measurements with the one obtained for the numeric Clarke channel model with $P = 30$ paths. This comparison is important because e.g. channel prediction based on sinusoidal modelling [3] shows poor performance for a small percentage of measured channel realizations, thus requiring outlier removal.

We demonstrate the robustness of ME band-limited prediction for LOS and non-LOS scenarios for a large number of measured vehicular channel realizations. No outlier removal was required. For non-LOS scenarios the predictor performs slightly worse than for Clarke's channel model measured in terms of the mean square prediction error at a prediction horizon of $\lambda/8$ and $3\lambda/8$. For LOS scenarios the ME energy band-limited predictor is able to take advantage of the reduced number of propagation paths and shows better performance than for Clarke's model.

9. ACKNOWLEDGEMENT

The authors thank KATHREIN-Werke KG for providing the base station antennas; J. A. Garcìa Naya, M. Šimko, and W. Schüttengruber for supporting us with the testbed measurements; and F. Kaltenberger for providing the Rice-factor estimation code.

The work of T. Zemen is supported by the Vienna Science and Technology Fund in the ftw. project COCOMINT. The work by S. Caban and M. Rupp has been funded by the Christian Doppler Laboratory for Wireless Technologies for Sustainable Mobility, the Institute of Communications and Radio Frequency Engineering, and KATHREIN-Werke KG. The Telecommunications Research Center Vienna (ftw.) is supported by the Austrian Government and the City of Vienna within the competence center program COMET.

REFERENCES

[1] T. Zemen, C. F. Mecklenbräuker, B. H. Fleury, and F. Kaltenberger, "Minimum-energy band-limited predictor with dynamic subspace selection for time-variant flat-fading channels," *IEEE Trans. Signal Processing*, vol. 55, no. 9, pp. 4535–4548, Sept. 2007.

[2] D. Slepian, "Prolate spheroidal wave functions, Fourier analysis, and uncertainty - V: The discrete case," *The Bell System Technical Journal*, vol. 57, no. 5, pp. 1371–1430, May-June 1978.

[3] M. Chen, T. Ekman, and M. Viberg, "New approaches for channel prediction based on sinusoidal modeling," *EURASIP J. Appl. Signal Process.*, vol. 2007, no. 1, pp. 1–13, 2007.

[4] M. Chen and M. Viberg, "Long-range channel prediction based on nonstationary parametric modeling," *IEEE Trans. Signal Processing*, vol. 57, no. 2, pp. 622–634, Feb. 2009.

[5] T. Zemen, C. F. Mecklenbräuker, J. Wehinger, and R. R. Müller, "Iterative joint time-variant channel estimation and multi-user detection for MC-CDMA," *IEEE Trans. Wireless Commun.*, vol. 5, no. 6, June 2006.

[6] T. Zemen and C. F. Mecklenbräuker, "Time-variant channel estimation using discrete prolate spheroidal sequences," *IEEE Trans. Signal Processing*, vol. 53, no. 9, pp. 3597–3607, September 2005.

[7] S. Beheshti and M. A. Dahleh, "A new information-theoretic approach to signal denoising and best basis selection," *IEEE Trans. Signal Processing*, vol. 53, no. 10, pp. 3613–3624, October 2005.

[8] S. Caban, C. Mehlführer, R. Langwieser, A. L. Scholz, and M. Rupp, "Vienna MIMO testbed," *EURASIP Journal on Applied Signal Processing*, vol. 2006, Article ID 54868, 2006.

[9] Kathrein, *Technical Specification Kathrein Antenna Type No. 800 10543*. [Online]. Available: http://www.kathrein-scala.com/catalog/80010543.pdf

[10] S. Caban, C. Mehlführer, G. Lechner, and M. Rupp, "'Testbedding' MIMO HSDPA and WiMAX," in *Proc. IEEE Vehicular Technology Conference (VTC 2009 Fall)*, Anchorage, AK, USA, Sep. 2009, submitted.

[11] L. J. Greenstein, D. G. Michelson, and V. Erceg, "Moment-method estimation of the Ricean K-factor," *IEEE Trans. Commun.*, vol. 3, no. 6, pp. 175–176, June 1999.

[12] I. M. Chakravarti, R. G. Laha, and J. Roy, *Handbook of methods of applied statistics*, ser. Wiley series in probability and mathematical statistics. John Wiley and Sons, 1967, vol. I.

[13] R. H. Clarke, "A statistical theory of mobile-radio reception," *Bell System Technical Journal*, p. 957, July-August 1968.